Hindawi
Mathematical Problems in Engineering
Volume 2021, Article ID 6688747, 11 pages
https://doi.org/10.1155/2021/6688747

Research Article

A New Heat Dissipation Model and Convective Two-Phase Nanofluid in Brittle Medium Flow over a Cone

Azad Hussain,[1] Qusain Haider,[1] Aysha Rehman,[1] Aishah Abdussattar,[1] and M. Y Malik[2]

[1]*Department of Mathematics, University of Gujrat, Gujrat 50700, Pakistan*
[2]*Department of Mathematics, College of Sciences, King Khalid University, Abha 61413, Saudi Arabia*

Correspondence should be addressed to Qusain Haider; qusain.haider336@gmail.com

Received 15 December 2020; Revised 18 February 2021; Accepted 28 September 2021; Published 23 October 2021

Academic Editor: Fateh Mebarek-Oudina

A time-dependent convectional flow of a two-phase nanofluid over a rotating cone with the impact of heat and mass rates is elaborated in this article. The instability in the flow field is induced by the cone angular velocity that depends on the time. The Navier–Stokes self-similar solution and the energy equations are obtained numerically. Here, the achieved solution is not only for Navier–Stokes equations but also for the equations of the boundary layers. In this work, the concentration, Brownian motion, and thermal buoyancy effects have important significance. We have assumed viscous dissipation with heat-absorbing fluid. Similarity answers for spinning cones with divider temperature boundary conditions give an arrangement of nonlinear differential conditions that have been handled numerically. The MATLAB methodology BVP4C is used to resolve the reduced structure of nonlinear differential equations numerically. Observation for skin friction and Nusselt number is also taken into account. Velocity and temperature impact is depicted graphically, while the outward shear stress values and heat allocation rate are included in tables.

1. Introduction

The design of reliable equipment in manufacturing industries relies heavily on convective flow ended a cone through radiative heat and form transfer. Due to its relevance in modern technology and applications in geothermal engineering, as well as other hydrological and astrophysical biofluid studies, researchers have shown a strong interest in heat and mass transfer in Newtonian flows in recent years. The analysis of fluid flow in a cone encompasses a wide variety of subjects. It is used in plastic processing, elastic sheet cooling, polymer technology, polymer chemistry, and engineering, to name a few. So, because of its enormous applications, the researchers are holding a purpose in this area. Dependence of viscosity on temperature plays a vital role in the realm of fluids flow. The viscosity of water decreases as the temperature increases, while the viscosity of gases rises as the temperature rises. The increase in temperature in lubricating fluids causes internal friction that affects the fluid's viscosity and will no longer remain constant. Because of this inadequacy, many researchers are interested to understand the effects of using different variable viscosity models.

Nanofluids remain a class of heat allocation fluids which caused suspended nanoparticles are distributed in the fluid (1–100 nm). In base fluids, locomotive oil, polymer solutions, bio-fluids, other critical fluids, water, and organic fluids (e.g., ethylene and diethylene) are commonly used. Nanoparticles are generally made of carbon in diverse edifices (e.g., carbon nanotubes, black lead, and diamond), metals (e.g., copper, hoary, and gold), and metal oxides (e.g., titanium and zirconia), besides functionalized nanoparticles. A wide-range of possible applications has been initiated for the use of nanofluids. Choi remained the first to research updraft conductivity development in nanofluids [1–12]. Nanofluids, bio and pharmacological nanofluids, remedial nanofluids, environmental nanofluids, and other heat transfer fluids are categorized according to their applications. Many researchers have looked into how extent, concentration, form, and other

assets affect the warmth transfer rate of a fluid. For the Prandtl number of airs, Hering and Grosh [13] investigated a steady mixed convection boundary layer flow from a vertical cone in an ambient fluid. For a broad range of Prandtl numbers, Himasekhar et al. [14] solved the similarity solution of the mixed convection boundary layer flow over a vertical rotating cone in an ambient fluid. Body solutions of unstable mixed convection flow from a rotating cone in a rotating fluid were obtained by Anil Kumar and Roy [15] a few years ago. Chamkha and Mudhaf [16] examined heat generation, consumption, and unstable heat and mass transfer from a revolving vertical cone with a magnetic field. Ravindran et al. [17] suggested a new approach for investigating the effects of fluid flow (suction/injection) on a vertical porous cone's steady natural convection boundary layer flow. The impact of heat-dependent viscosity with viscous heat generation on third-grade fluid flow in a standard pipe was examined by Nadeem and Hussain [18]. Exploitation the finite simple difference method, numerical solutions were obtained. Different fluids like water, ethylene glycol, and oil, due to their poor thermal conductivity, have low heat transfer properties. It is now realized that by retaining nano-sized metal flakes such as Al, titanium, silver, gold, Cu, or their oxides, the thermophysical characteristics of such fluids could be enhanced, ending in what is commonly known as nanofluid [19]. Several researchers have spent the last few years studying the edge layer movement of nanofluid fluids in various geometries and under various conditions. Kameswaran et al. [20] investigated the flow of hydromagnetic nanofluids due to a shrinking surface. Over a stretching field, Kameswaran et al. [21] discovered solutions for the deflation-point flow equations. Fauzi et al. [22] explored the time-independent nanofluid boundary film flowing along a perpendicular cone in a brittle medium. Boutra et al. [23] investigated unrestricted convection induction in a nanofluid-filled framework through round heaters, and Ambethkar and Kumar [24] investigated 2D noncompressible flow solutions with the transfer of heat in a powered square cavity singing stream function-vorticity model. Cheng [25] addressed natural convection flowing through a formatted cone in a brittle medium in the boundary layer. Chamkha et al. [26] examined the issue of mixed convection boundary layer flow in a continuous, turbulent flow over a rigid cone enclosed in a brittle thermal radiation medium. Nadeem and Saleem [27] examined turbulent nanofluid flow in a turning cone subjected to an induced magnetic field. In this paper, we look at a two-phase nanofluid flow along a vertically stretching cone.

The work of Heiring and Grosh [28] on natural convection over a multi-isothermal cone is one of the most recent cone-shaped surface boundary layer studies. A theoretical study of forced convection flow in relation to a rotating cone was suggested by Tien and Tsuji [29]. Koh and Price [30] have evaluated the transfer of heat past a pivoting cone. Ellahi et al. [31] have studied the analysis of simplified third-grade slide Couette fluid flow. There are some related studies about this phenomenon provided in References [32–43]. Extrusion processes, plastic product processing, polymers, and silicone slips, wire and copper-coating, glass and fiber optic production, hot spinning manufacture, metal rolling, food preparation, and a variety of other topics are frequently mentioned.

The combination of fluids has a broad range of applications, including cooling systems, heating processes, as well as biomedical and automotive science and technologies that control heat and mass transfer rates. The persistence of this article is to inspect the flow of liquid-based two-phase nanofluids (copper oxide and silver added to water) over a rotating cone. Two-phase flows include the flows that transition from pure liquid to vapor as a result of external heating, separated flows, and scattered two-phase flows in which phase is observed in a continuous carrier phase in the form of particles, droplets, or leaks. We have solved governing differential equations with the assistance of the BVP4V scheme under MATLAB. It also describes the possessions of relevant bodily parameters that affect the velocities, surface strain tensors, temperature, and convection rate with the help of graphs and tables.

2. Mathematical Formulations

We deliberate the flow of a compressible viscous nanofluid along an erect turning cone enclosed in a brittle medium as a two-dimensional time-dependent boundary layer. Figure 1 displays the scheme of coordinates and the corporal model. We have used a rectangular coordinate system in which the x–axis is determined along a meridian, the y–axis is determined along a round section, and the z–axis is determined on the cone's surface. Let u, v, and w be velocity gears, with x (tangential), y (azimuthal), and z (horizontal) orders (normal). The equations can be written as follows:

$$u + \frac{x}{\partial z}\frac{\partial u}{\partial z} + x\frac{\partial w}{\partial z} = 0, \tag{1}$$

$$\frac{\partial u}{\partial t} + u\frac{\partial u}{\partial x} + \frac{w\partial u}{\partial z} - \frac{v^2}{x} = \frac{\nu_{nf}\partial^2 u}{\partial z^2} - \frac{v_e^2}{x} + g\zeta\cos\alpha^*(T - T_\infty), \tag{2}$$

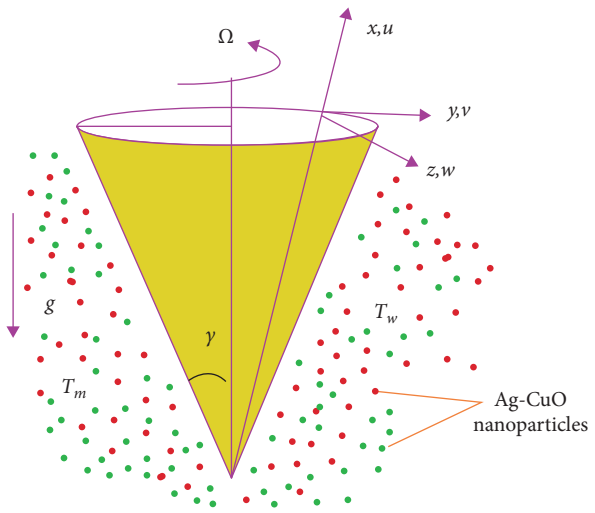

Figure 1: Bodily geometry of the problem.

$$\frac{\partial v}{\partial t}+\frac{u\partial v}{\partial x}+w\frac{\partial v}{\partial z}+u\frac{v}{x}=\frac{\partial v_e}{\partial t}+\nu_{\mathrm{nf}}\frac{\partial^2 v}{\partial z^2}, \tag{3}$$

$$u\frac{\partial T}{\partial x}+\frac{\partial T}{\partial t}+w\frac{\partial T}{\partial z}=\alpha_{\mathrm{nf}}\frac{\partial^2 T}{\partial z^2}. \tag{4}$$

The boundaries conditions are set, subject to initial terms and conditions as follows:

$$\begin{aligned} &u(0,x,z)=v=w=u_i,\\ &v_i w_i,\\ &T=T_i,\\ &u(t,0,z)=w=0,\\ &v=\frac{\Omega_1 x\ \sin\alpha^*}{1-st^*},\\ &T=T_W. \end{aligned} \tag{5}$$

Reference [15] provides the momentum, temperature, initial conditions, and boundary conditions for this issue.

The following transformation is defined where A is the Deborah number and γ_1 and γ_2 are the buoyancy parameters. The things of physical importance use in the two-phase model are as follows: α_{nf} is the thermal diffusivity, ν_{nf} is the kinematic viscosity, μ_{nf} is the effective dynamic viscosity, ρ_{nf} is the density, (ρC_P)nf is the heat capacity, κ_{nf} is the nanofluid thermal conductivity, and $(\rho\beta)_{\mathrm{nf}}$ is the nanofluid thermal expansion coefficient:

$$\begin{aligned} \eta&=\frac{(x\Omega\sin\alpha^*)^{0.5}z}{\nu(1-st^*)^{0.5}},\\ v_e&=\frac{x\Omega_2\sin\alpha^*}{1-st^*},\\ \alpha&=\frac{\Omega_1}{\Omega},\\ t^*&=\Omega\sin\alpha^* t,\\ w&=\frac{(\sin\alpha^*)^{1/2}(\nu\Omega)^{1/2}f(\eta)}{(1-st^*)^{1/2}},\\ T-T_\infty&=(T_W-T_\infty)\theta(\eta),\\ u(t,x,z)&=-\frac{2^{-1}\sin\alpha^* f'\Omega x}{1-st^*},\\ v&=\Omega x\ \sin\alpha^{*\,1/2}_{(1-st^*)}g(\eta),\\ T_W-T_\infty&=\frac{(T_0-T_\infty)xL^{-1}}{(1-st^*)^2},\\ Gr_1&=\frac{\cos\alpha^*(T_0-T_\infty)g\beta L^3}{\nu^2},\\ \gamma_1&=\frac{Gr_1}{\mathrm{Re}_L^2},\\ \mathrm{Re}_L&=\sin\alpha^*\Omega L^2\nu^{-1},\\ \mathrm{Pr}&=\frac{\nu}{\alpha}. \end{aligned} \tag{6}$$

$$\begin{aligned} \nu_{\mathrm{nf}}&=\frac{\mu_{\mathrm{nf}}}{\rho_{\mathrm{nf}}},\\ \alpha_{\mathrm{nf}}&=\frac{k_{\mathrm{nf}}}{(\rho c_p)_{\mathrm{nf}}},\\ \mu&=\mu_f(1-\phi)^{-2.5},\\ \rho_{\mathrm{nf}}&=(1-\phi)*\rho_f+\phi\rho_s,\\ &(\rho c_p)_{\mathrm{nf}},\\ \rho_f&=(1-\phi)*(c_p\rho)_f+\phi(\rho c_p)_f,\\ \frac{k_{\mathrm{nf}}}{k_f}&=\frac{\left((k_s+2k_f)-2\phi(k_f-k_s)\right)}{\left(k_s+2k_f+\phi(k_f-k_s)\right)},\\ (\rho\beta)_{\mathrm{nf}}&=(1-\phi)(\rho\beta)_f+\phi(\rho\beta)_s. \end{aligned} \tag{7}$$

The transformation's equations (7) and (6) are replaced into (1)–(3). After that equation (1) will be fulfilled automatically, and equations (2)–(4) diminish to the form as follows:

$$\left(\frac{f'''}{(1-\phi)^{2.5}\left(1-\phi+\phi\left(\rho_s/\rho_f\right)\right)}-\left(f+\frac{1}{2}s\eta\right)f'+\left(\frac{1}{2}f'-s\right)f'-2\left(g-(1-\alpha_1)^2\right)-2\gamma_1\theta\right),$$

$$\left(\frac{g''}{(1-\phi)^{2.5}\left(1-\phi+\phi\left(\rho_s/\rho_f\right)\right)}-(-f'g+fg')+s\left(1-\alpha_1-g-\frac{1}{2}\eta g'\right)\right), \tag{8}$$

$$\left(\frac{1}{\Pr}\left(\frac{\kappa_{\mathrm{nf}}}{\kappa_f}\right)\theta''-\left(f\theta'-\frac{f'\theta}{2}\right)-2s\theta+\frac{1}{2}s\eta\theta'\right).$$

Now, the boundary conditions are

$$\begin{aligned} f(0)&=0,\\ g(\infty)&=-1+\alpha_1,\\ g(0)&=\alpha_1,\\ \theta(0)&=-1,\\ f\prime(\infty)&=0,\\ f\prime(0)&=0,\\ \theta(\infty)&=0. \end{aligned} \tag{9}$$

The skin friction C_{fx} across the x-axis, C_{fy} along y-axis, and Nusselt sum Nu_x are physical quantities of our distinct interest where

$$\begin{aligned} C_{fx}&=-\mathrm{Re}_x^{-(1/2)}\left(\frac{2\mu\ \partial u}{\partial z}\right)_{z=0},\\ C_{fy}&=\left(\frac{2\mu\ \partial v}{\partial z}\right)_{z=0}\left(-\mathrm{Re}_x^{-(1/2)}\right), \end{aligned} \tag{10}$$

or in the form of dimensionless

$$\begin{aligned} C_{fx}\mathrm{Re}_x^{1/2}&=(-f'')_{\eta=0},\\ C_{fy}\mathrm{Re}_x^{1/2}&=(-g\prime)_{\eta=0}. \end{aligned} \tag{11}$$

In dimensionless form, the heat transfer coefficient is given as

$$\mathrm{Nu}_x\mathrm{Re}_x^{1/2}=-\theta\prime(0). \tag{12}$$

Now, the Reynolds number is

$$Re_x=\frac{x^2\sin\ st}{\nu}. \tag{13}$$

3. Numerical Solution

The numerical technique performs the solutions of the joined linear sinusoidal differential equations. The following initial estimates and nonlinear operators are f_0, g_0, and θ_0, respectively, for velocity components and temperature fields.

New variables are defined simplifying differential equations of high order in the form of first-order equation, i.e.,

$$\begin{aligned} F&=y_1,\\ \rho_f&=b,\\ f'&=y_2,\\ g&=y_4,\\ F''&=y_3,\\ \rho_s&=a,\\ g'&=y_5,\\ g''&=y_5',\\ F'''&=y_3',\\ \theta(0)&=y_6,\\ \theta'&=y_7,\\ \theta''&=y_7',\\ k_s&=m,\\ k_f&=n,\\ \left(\rho c_p\right)_s&=c,\\ \left(\rho c_p\right)_f&=d. \end{aligned} \tag{14}$$

Now, the new equations are

$$\begin{aligned} y_3'&=\left[\left[(1-\phi)^{2.5}\left(1-\phi+\frac{\phi a}{b}\right)\right]\left[\left(y(1)y(3)+\frac{1}{2}xsy(3)\right)-\frac{1}{2}y^2(2)+sy(2)\right)+2y^2(4)-(1-\alpha_1)^2+2\gamma_1y(6)\right],\\ y_5'&=\left[(1-\phi)^{2.5}\left(1-\phi+\frac{\phi a}{b}\right)\right]\left[y(1)y(5)-y(4)y(2)\left(-s+s\alpha_1+sy(4)+\frac{1}{2}sxy(5)\right)\right],\\ y_7'&=\left[\frac{(m+2)(n+2)\phi\ (n-m)}{(m+2)(n-2)\phi\ (n-m)}\right]\left[Pry(7)y(1)-\frac{y(6)y(2)}{2}\left(2sy(6)-\frac{Pr1}{2}sxy(7)\right)\right]. \end{aligned} \tag{15}$$

Along with limitation,

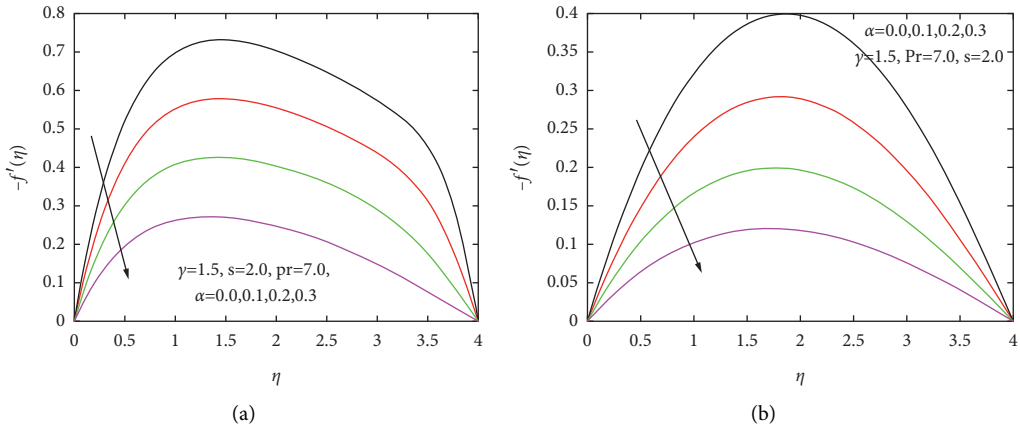

FIGURE 2: (a) Impact of α_1 on the velocity distribution $-f\prime(n)$ for Cuo nanoparticles. (b) Impact of α_1 on the velocity distribution $-f\prime(n)$ for Ag nanoparticles.

$$\begin{aligned} y(1) &= 0, \\ y(6) &= -1, \\ y_\infty(2) &= 0, \\ y(2) &= 0, \\ y(4) &= \alpha_1, \\ y_\infty(6) &= 0. \end{aligned} \tag{16}$$

4. Graphical Observations and Discussion

This section of the learning includes the graphical and mathematical outcomes of multiple major parameters on velocities, temperature, coefficients of surface stress, and coefficient of heat transfer. Such variations are noted in figures. Figures 2(a) and 2(b) and Figures 3(a) and 3(b) are sketched to demonstrate primary velocity activity for parameter mixed convection. The positive parameter of buoyancy functions as a desirable gradient of pressure is mended to improve the property of the fluid. It is foretold from Figures 2(a) and 2(b) and Figures 3(a) and 3(b) that the thickness of the upper and lower layers will decrease with increase in α_1 and γ_1 values; further, the primary velocity will have a higher magnitude for γ_1. The effect of mixed convection on buoyancy parameter γ_1 is to decrease the secondary velocity g (see Figures 4(a) and 4(b), respectively). The secondary velocity g is also seen to have the greater magnitude for α_1. A vertically spinning or expanding cone was analyzed on the unstable frontier layer flow of both water-based nanofluids. The flow was contrary to viscous debauchery, the cohort of excess heat, and a natural process. The numerical technique is used to resolve the equations. We studied the belongings on the nanofluid velocity (f&g) and temperature (θ) profiles and even the skin friction (C_{fx}&C_{fy}) coefficient, energy, and mass exchange coefficients of the nanoparticle volume segment, buoyancy parameter γ_1, heat production, and chemical reaction. We considered nanoparticles of copper oxide (Cuo) and silver (Ag) with water as the basis fluid. In Figures 2(a) and 2(b) and Figures 3(a) and 3(b), see the variation of the angular velocity ratio α_1, and the buoyancy coefficient γ_1 on tangential velocity $-f\prime$ is plotted. Tangential velocities are observed to decrease for α_1 and γ_1 parameters. Figures 4(a) and 4(b) display the variance of the angular velocity ratio α_1 on azimuthal velocity g. At g, the action of α_1 is contrary to that of tangential velocity $-f\prime$. Here, Figures 5(a) and 5(b) are shown in the temperature sector θ for specific Pr values. The width of the thermoelectric boundary layer is indicated to reduce for rising Pr values. This is because the higher Prandtl number fluid has more heat conductivity resulting in a softer heat boundary layer. Now, see in Cuo case Figure 5(a) temperature decrease with increases the value of Pr but contrary in Ag case Figure 5(b). Figures 6(a) and 6(b) address the variance in the ratio of the γ_1 buoyancy parameter on the secondary velocity skin friction coefficient. Skin values decrease in Cuo case but enhance in Tio_2 case. Figures 7(a) and 7(b) show changes in the coefficient of C_{fy} skin friction by rising α_1. Figure 7(a) shows that C_{fy} values increase in Cuo but Figure 7(b) shows decline values of C_{fy}. Physically, we can conclude that the surface temperature is higher than the fluid temperature close to the cone boundaries; therefore, larger γ_1 gives the greater values of skin friction. It is examined that the coefficient of tangential skin friction (C_{fx}&C_{fy}) decreases as α_1 increases (see Figures 7(a) and 7(b)). Figures 8(a) and 8(b) and Figures 9(a) and 9(b) show that the primary skin friction coefficients increase or decrease with the rise in α_1, also the same behavior for γ_1. In Figures 8(a) and 9(a), C_{fy} values decline for Cuo, and we see that in Figures 8(b) and 9(b), the values of C_{fx} are enhanced when the values of α_1 and γ_1 are increased. Since the impact of Pr in the primary $-f'$ and secondary g directions on the velocity profiles is relatively small, therefore, the profiles are ignored. In Figures 10(a) and 10(b), the heat exchange rate has decreased, with increase in Pr. In Figures 10(a) and 10(b), see that the Nusselt number decreases when the values of Pr increase. Finally, figures also display the positive impact of heat dissipation on the local

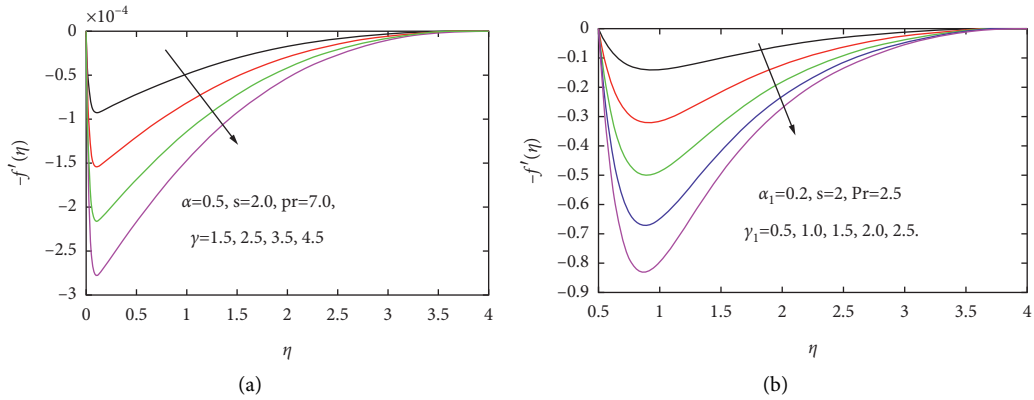

Figure 3: (a) Impact of γ_1 on velocity distribution $-f\prime$ for Cuo nanoparticles. (b) Impact of γ_1 on velocity distribution $-f\prime$ for Ag nanoparticles.

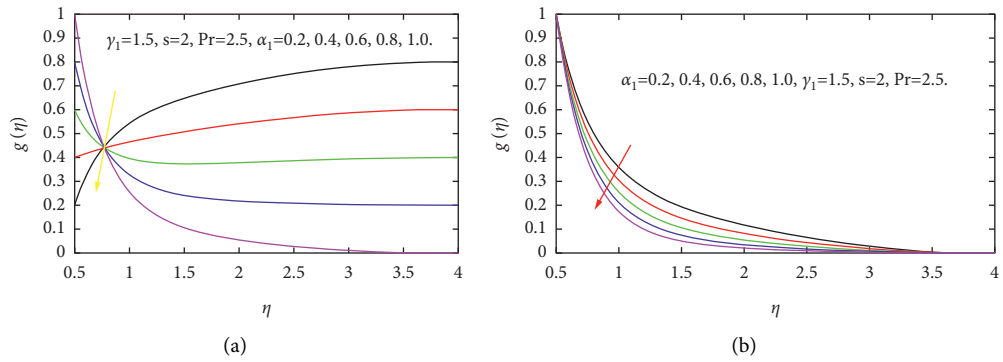

Figure 4: (a) Impact of α_1 on velocity profile $g(\eta)$ for Cuo nanoparticles. (b) Impact of α_1 on velocity profile $g(\eta)$ for Ag nanoparticles.

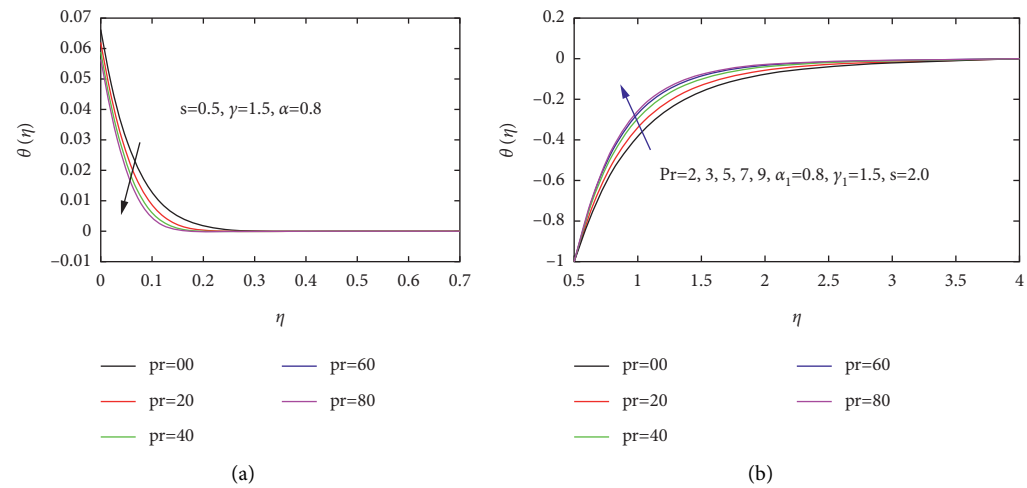

Figure 5: (a) Deviation of Pr on temperature profile $\theta(\eta)$ for Cuo nanoparticles. (b) Deviation of Pr on temperature profile $\theta(\eta)$ for Ag nanoparticles.

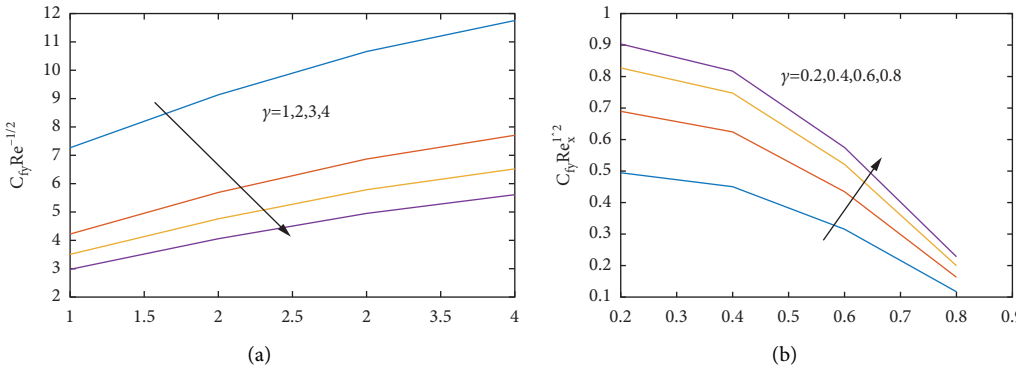

FIGURE 6: (a) Impact on skin friction C_{fy} along y-direction of γ_1 for Cuo nanoparticles. (b) Impact on skin friction C_{fy} along y-direction of γ_1 for Ag nanoparticles.

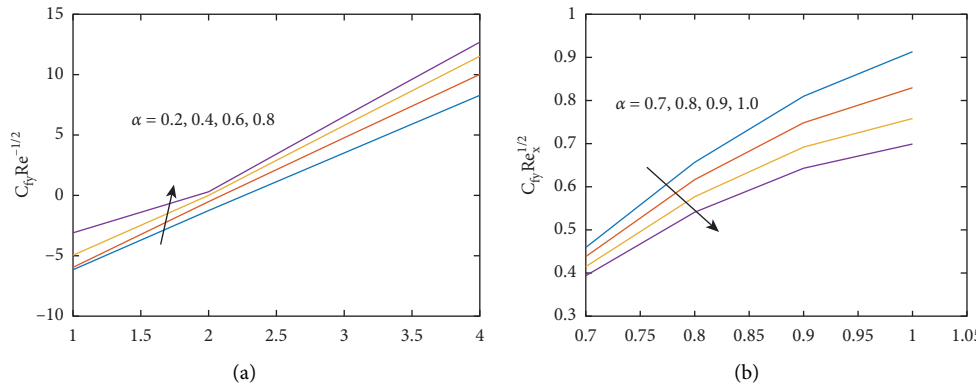

FIGURE 7: (a) Impact on skin friction of α_1 besides y-direction for Cuo – water. (b) Impact on skin friction of α_1 besides y-direction for Ag – water.

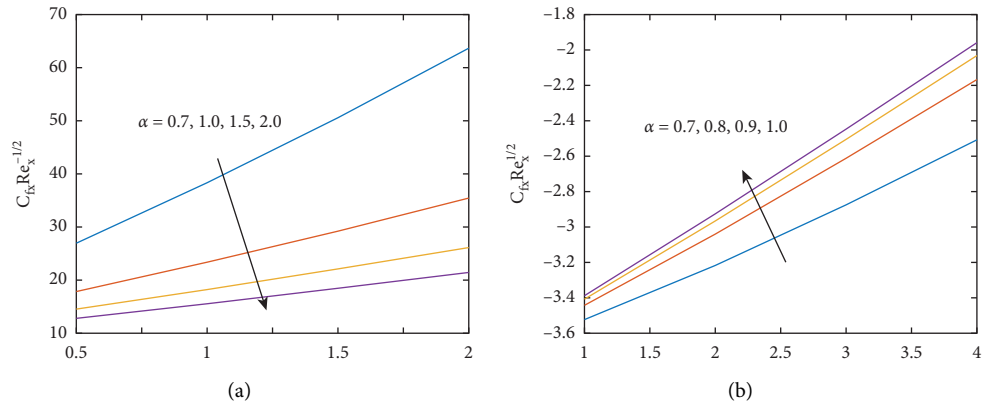

FIGURE 8: (a) Influence on skin friction C_{fx} along x-direction of α_1 for Cuo – water. (b) Influence on skin friction C_{fx} along x-direction of α_1 forAg – water

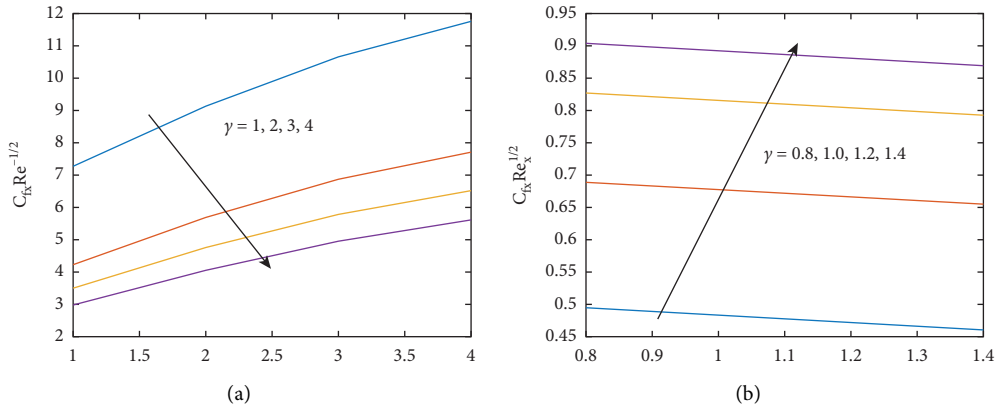

Figure 9: (a) Influence on skin friction of γ_1 along y-direction for Cuo – water. (b) Influence on skin friction of γ_1 along y-direction for Ag – water.

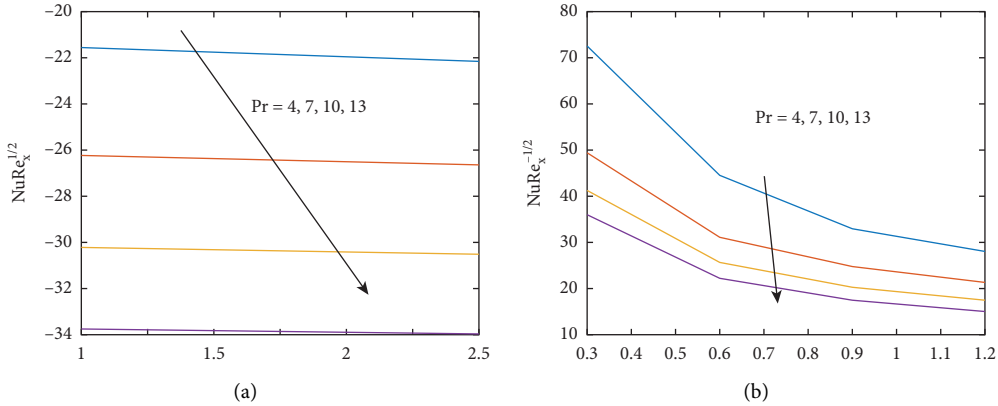

Figure 10: (a) Impact on the Nusselt number of Pr for Cuo – water of nanoparticles. (b) Impact on the Nusselt number of Pr for water Ag of nanoparticles.

Table 1: Variations of $\alpha, \gamma, \mathbf{s}$, and **Pr** on the coefficient of skin friction $\mathbf{C_{fx}}$ and $\mathbf{C_{fy}}$ and local Nusselt number ($\mathbf{Nu_x}$) for **Cuo – water**.

α_1	γ_1	s	Pr	C_{fx}	C_{fy}	Nu_x
0.5	1.5	2.0	1.0	0.56971	0.64524	−33.7303
	2.5			0.55597	0.61825	−33.8036
	3.5			0.54147	0.59124	−33.8762
	4.5			0.52733	0.56420	−33.9481
0.8				0.75065	0.35930	−65.5158
1.0	2.5	0.8	2.5	0.73655	0.55678	−65.6143
1.2				0.72245	0.81300	−65.7122
1.4				0.70835	0.86329	−65.8094
		0.6		0.55559	0.54225	−71.2271
		0.8		0.54147	0.52817	−71.1483
		1.0		0.52735	0.51408	−71.1877
1.2	2.5	1.2	3.5	0.51323	0.50000	−71.1087
			1.0	−21.5615	−26.2363	−30.2121
			1.5	−21.7700	−26.3719	−30.3089
1.2	3.5	1.0	2.0	−21.9711	−26.5047	−30.4045
			2.5	−22.1854	−26.1654	−30.4988

Nusselt number. It must be noted that the shape effects in all figures are positive and growing factor in the ratio of heat flow. Table 1 and Table 2 represent the variations of α_1, γ_1, s, and Pr on the coefficient of skin friction (C_{fx}&C_{fy}) and local Nusselt number (Nu_x). Table 3 shows the physical properties of copper oxide and silver.

Table 2: Effects of the parameter on skin friction and Nusselt number for **Ag – water**.

α_1	γ_1	s	Pr	C_{fx}	C_{fy}	Nu_x
0.5	1.5	2.0	1.0	0.160744	0.161692	−33.7303
	2.5			0.159905	0.164064	−33.8036
	3.5			0.161692	0.166214	−33.8762
	4.5			0.161762	0.161692	−33.9481
0.8				0.161825	0.161568	−65.5158
1.0	2.5	0.8	2.5	0.161692	0.161442	−65.6143
1.2				0.160717	0.161692	−65.7122
1.4				1.159742	0.162193	−65.8094
		0.6		0.161692	0.863293	−71.2271
		0.8		0.227089	0.542258	−71.1483
		1.0		0.292715	0.528174	−71.1877
1.2	2.5	1.2	3.5	0.161692	0.514088	−71.1087
			1.0	0.093331	0.500001	−30.2121
			1.5	0.032939	−26.2363	−30.3089
1.2	3.5	1.0	2.0	0.161692	−26.3719	−30.4045
			2.5	0.039527	−26.5047	−30.4988

Table 3: Base fluid and nanoparticles have thermophysical characteristics.

Physical properties	C_P	ρ	κ
H_2o	4179	997.1	0.613
Cuo	531.80	6320	76.50
Ag	235	10500	429

5. Concluding Remarks

\In this numerical study, we have considered an unstable two-phase nanofluid flow and heat transfer attitudes over a cone littered with two diverse metal types specifically Ag and Cuo. Unsteady mixed convection flow has been investigated in a moving viscous fluid on a turning cone. Numerical solution of ordinary differential equations BVP4C has been implemented successfully. The afresh determined outcomes are recognized to be accessible in the literature in traditional agreement with the findings previously reported. Viscous dissipation was found to have the consequence of swelling the nanofluid temperature within the gravity effects area when the heat transfer rate from the layer decreases with an increase in a viscous heat generation. The analysis summary is as follows:

(1) For increasing γ_1 and α_1, the tangential velocity field $-f'$ declines. However, s near to the boundary often causes $-f\prime$ to decrease and increases it far away from the boundary for increasing γ_1 and α_1.

(2) On elevating α_1, the azimuthal velocity field g decreases and decreases with increase in s.

(3) For higher values of Pr, the temperature profile $\theta(\eta)$ increases for Ag but decreases for Cuo.

(4) Growing the importance of shape effects has raised the temperature profile and also the local Nusselt number.

(5) The two-phase nanoparticle model has always a bigger impact than nanoparticles on the temperature profile.

List of Symbols

Pr: Prandtl number
T: Temperature
C_{fx}: In the x-direction, there is local skin friction
C_{fy}: Skin friction in y-direction
f, g: The velocity of a dimensionless stream function component in $x-$ and $y-$direction, respectively
K, L: Thermal conductivity and area of the indentation, respectively, $\mathrm{Km^{-1}K^{-1}}$
μ: Dynamic viscosity $\mathrm{Nms^{-2}}$
Nu_x: Local Nusselt number
Re_x: Reynold number based on x
Re_L: Reynold number based on L
$(\rho C_p)_{nf}$: Heat capacity of nanofluid jk^{-1}
(u, v, w): Velocity components $\mathrm{ms^{-1}}$
t, t^*: Dimensional and dimensionless times, respectively
(x, y, z): The distance measured along the meridian of a circular segment parallel to the cone's superficial
α: Semiupright angle of the cone
η: Similarity variable
θ: Dimensionless temperature
γ_1: Buoyancy parameter due to temperature
ν: Kinematic viscosity $\mathrm{m^2s^{-1}}$
ρ: Density $\mathrm{kgm^{-3}}$
ρ_{nf}: Nanofluid density $\mathrm{kgm^{-3}}$
μ_f: The viscosity of fluid $\mathrm{Nms^{-2}}$
μ_{nf}: Nanofluid viscosity $\mathrm{Nms^{-2}}$
α_{nf}: Nanofluid thermal diffusivity $\mathrm{m^2s^{-1}}$.

Data Availability

The data used to support the findings of the study are available from the corresponding author upon request.

Conflicts of Interest

The authors declare that they have no conflicts of interest.

Acknowledgments

The authors extend their appreciation to the Deanship of Scientific Research at King Khalid University, Abha 61413, Saudi Arabia for funding this work through Research Groups Program under grant number R.G.P-1/223/42.

References

[1] S. U. S. Choi, "Enhancing thermal conductivity of a fluids with nanoparticles," *ASME Int*, vol. 66, pp. 99–105, 1995.

[2] S. Chen, M. K. Hassanzadeh-Aghdam, and R. Ansari, "An analytical model for elastic modulus calculation of SiC whisker-reinforced hybrid metal matrix nanocomposite containing SiC nanoparticles," *Journal of Alloys and Compounds*, vol. 767, pp. 632–641, 2018.

[3] X. Wang, J. Wang, X. Sun et al., "Hierarchical coral-like NiMoS nanohybrids as highly efficient bifunctional electrocatalysts for overall urea electrolysis," *Nano Research*, vol. 11, no. 2, pp. 988–996, 2018.

[4] M. R. Eid and A. F. Al-Hossainy, "Combined experimental thin film, DFT-TDDFT computational study, flow and heat transfer in [PG-MoS2/ZrO2]C hybrid nanofluid," *Waves in Random and Complex Media*, pp. 1–26, 2021.

[5] P. Wang, X. Zhang, W. Duan, W. Teng, Y. Liu, and Q. Xie, "Superhydrophobic flexible supercapacitors formed by integrating hydrogel with functional carbon nanomaterials," *Chinese Journal of Chemistry*.

[6] M. Wang, M. Hu, B. Hu et al., "Bimetallic cerium and ferric oxides nanoparticles embedded within mesoporous carbon matrix: electrochemical immunosensor for sensitive detection of carbohydrate antigen 19-9," *Biosensors and Bioelectronics*, vol. 135, pp. 22–29, 2019.

[7] Y. Liu, Q. Zhang, M. Xu et al., "Novel and efficient synthesis of Ag-ZnO nanoparticles for the sunlight-induced photocatalytic degradation," *Applied Surface Science*, vol. 476, pp. 632–640, 2019.

[8] H. Alotaibi, S. Althubiti, M. R. Eid, and K. L. Mahny, "Numerical treatment of mhd flow of casson nanofluid via convectively heated non-linear extending surface with viscous dissipation and suction/injection effects," *Computers, Materials & Continua*, vol. 66, no. 1, pp. 229–245, 2020.

[9] W.-C. Tzeng, P.-Y. Su, N.-S. Tzeng, C.-B. Yeh, T.-H. Chen, and C.-H. Chen, "A moral life after a suicide death in Taiwan," *Qualitative Health Research*, vol. 20, no. 7, pp. 999–1007, 2010.

[10] M. Ferdows, M. D. Shamshuddin, S. O. Salawu, and K. Zaimi, "Numerical simulation for the steady nanofluid boundary layer flow over a moving plate with suction and heat generation," *SN Applied Sciences*, vol. 3, no. 2, pp. 1–11, 2021.

[11] A. A. Alaidrous and M. R. Eid, "3-D electromagnetic radiative non-Newtonian nanofluid flow with Joule heating and higher-order reactions in porous materials," *Scientific Reports*, vol. 10, no. 1, pp. 14513–14519, 2020.

[12] A. F. Al-Hossainy and M. R. Eid, "Structure, DFT calculations and heat transfer enhancement in [ZnO/PG + H2O]C hybrid nanofluid flow as a potential solar cell coolant application in a double-tube," *Journal of Materials Science: Materials in Electronics*, vol. 31, no. 18, pp. 15243–15257, 2020.

[13] R. G. Hering and R. J. Grosh, "Laminar free convection from a non-isothermal cone," *International Journal of Heat and Mass Transfer*, vol. 5, no. 11, pp. 1059–1068, 1962.

[14] K. Himasekhar, P. K. Sarma, and K. Janardhan, "Laminar mixed convection from a vertical rotating cone," *International Communications in Heat and Mass Transfer*, vol. 16, no. 1, pp. 99–106, 1989.

[15] D. Anilkumar and S. Roy, "Unsteady mixed convection flow on a rotating cone in a rotating fluid," *Applied Mathematics and Computation*, vol. 155, no. 2, pp. 545–561, 2004.

[16] A. J. Chamkha and A. Al-Mudhaf, "Unsteady heat and mass transfer from a rotating vertical cone with a magnetic field and heat generation or absorption effects," *International Journal of Thermal Sciences*, vol. 44, no. 3, pp. 267–276, 2005.

[17] R. Ravindran, S. Roy, and E. Momoniat, "Effects of injection (suction) on a steady mixed convection boundary layer flow over a vertical cone," *International Journal of Numerical Methods for Heat and Fluid Flow*, vol. 19, no. 3/4, pp. 432–444, 2009.

[18] S. Nadeem, A. Hussain, and M. K, "Stagnation flow of a Jeffrey fluid over a shrinking sheet," *Zeitschrift für Naturforschung A*, vol. 65, no. 6-7, pp. 540–548, 2010.

[19] S. U. S. Choi and J. A. Eastman, "Enhancing thermal conductivity of fluids with nanoparticles, San Francisco," *ASME International Mechanical Engineering Congress and Exposition*, vol. 231, pp. 99–103, 1995.

[20] P. K. Kameswaran, M. Narayana, P. Sibanda, and P. V. S. N. Murthy, "Hydromagnetic nanofluid flow due to a stretching or shrinking sheet with viscous dissipation and chemical reaction effects," *International Journal of Heat and Mass Transfer*, vol. 55, no. 25-26, pp. 7587–7595, 2012.

[21] P. K. Kameswaran, P. Sibanda, C. Ramreddy, and P. V. Murthy, "Dual solutions of stagnation-point flow of a nanofluid over a stretching surface," *Boundary Value Problems*, vol. 2013, no. 1, pp. 1–12, 2013.

[22] E. L. A. Fauzi, S. Ahmad, and I. Pop, "Mixed convection boundary layer flow from a vertical cone in a porous medium filled with a nanofluid," *Engineering and Technology*, vol. 6, pp. 15–18, 2012.

[23] A. Boutra, K. Ragui, N. Labsi, and Y. Benkahla, "Free convection enhancement within a nanofluid' filled enclosure with square heaters," *International Journal of Heat and Technology*, vol. 35, no. 3, pp. 447–458, 2017.

[24] V. Ambethkar and M. Kumar, "Numerical solutions of 2-D unsteady incompressible flow with heat transfer in a driven square cavity using streamfunction-vorticity formulation," *International Journal of Heat and Technology*, vol. 35, no. 3, pp. 459–473, 2017.

[25] C.-Y. Cheng, "Natural convection boundary layer flow over a truncated cone in a porous medium saturated by a nanofluid," *International Communications in Heat and Mass Transfer*, vol. 39, no. 2, pp. 231–235, 2012.

[26] A. J. Chamkha, S. Abbasbandy, A. M. Rashad, and K. Vajravelu, "Radiation effects on mixed convection about a cone embedded in a porous medium filled with a nanofluid," *Meccanica*, vol. 48, no. 2, pp. 275–285, 2013.

[27] S. Nadeem and S. Saleem, "Unsteady mixed convection flow of nanofluid on a rotating cone with magnetic field," *Applied Nanoscience*, vol. 4, no. 4, pp. 405–414, 2014.

[28] R. G. Hering and R. J. Grosh, "Laminar combined convection from a rotating cone," *Journal of Heat Transfer*, vol. 85, no. 1, pp. 29–34, 1963.

[29] C. L. Tien and I. J. Tsuji, "A theoretical analysis of laminar forced flow and heat transfer about a rotating cone," *Journal of Heat Transfer*, vol. 87, no. 2, pp. 184–190, 1965.

[30] J. C. Y. Koh and J. F. Price, "Nonsimilar boundary-layer heat transfer of a rotating cone in forced flow," *Journal of Heat Transfer*, vol. 89, no. 2, pp. 139–145, 1967.

[31] R. Ellahi, T. Hayat, and F. M. Mahomed, "Generalized Couette flow of a third-grade fluid with slip: the exact solutions," *Zeitschrift für Naturforschung A*, vol. 65, no. 12, pp. 1071–1076, 2010.

[32] R. Ellahi, T. Hayat, F. M. Mahomed, and S. Asghar, "Effects of slip on the non-linear flows of a third grade fluid," *Nonlinear Analysis: Real World Applications*, vol. 11, no. 1, pp. 139–146, 2010.

[33] O. D. Makinde, "Computational modelling of MHD unsteady flow and heat transfer toward a flat plate with Navier slip and Newtonian heating," *Brazilian Journal of Chemical Engineering*, vol. 29, no. 1, pp. 159–166, 2012.

[34] M. R. Hajmohammadi and S. S. Nourazar, "On the insertion of a thin gas layer in micro cylindrical Couette flows involving power-law liquids," *International Journal of Heat and Mass Transfer*, vol. 75, pp. 97–108, 2014.

[35] M. R. Hajmohammadi, S. Salman Nourazar, and A. Campo, "Analytical solution for two-phase flow between two rotating cylinders filled with power law liquid and a micro layer of gas," *Journal of Mechanical Science and Technology*, vol. 28, no. 5, pp. 1849–1854, 2014.

[36] W. A. Khan, Z. H. Khan, and M. Rahi, "Fluid flow and heat transfer of carbon nanotubes along a flat plate with Navier slip boundary," *Applied Nanoscience*, vol. 4, no. 5, pp. 633–641, 2014.

[37] M. Qasim, Z. H. Khan, W. A. Khan, and I. Ali Shah, "MHD boundary layer slip flow and heat transfer of ferrofluid along a stretching cylinder with prescribed heat flux," *PLoS One*, vol. 9, no. 1, Article ID e83930, 2014.

[38] A. Hussain, A. Rehman, S. Nadeem et al., "A Combined Convection Carreau–Yasuda Nanofluid Model over a Convective Heated Surface Near a Stagnation Point: A Numerical Study," *Mathematical Problems in Engineering*, vol. 2021, Article ID 6665743, 14 pages, 2021.

[39] M. Y. Malik, A. Hussain, and S. Nadeem, "Analytical treatment of an oldroyd 8-constant fluid between coaxial cylinders with variable viscosity," *Communications in Theoretical Physics*, vol. 56, no. 5, pp. 933–938, 2011.

[40] M. Y. Malik, I. Khan, A. Hussain, and T. Salahuddin, "Mixed convection flow of MHD Eyring-Powell nanofluid over a stretching sheet: a numerical study," *AIP Advances*, vol. 5, no. 11, p. 117118, 2015.

[41] D. Anilkumar and S. Roy, "Unsteady mixed convection flow on a rotating cone in a rotating fluid," *Applied Mathematics and Computation*, vol. 155, no. 2, pp. 545–561, 2004.

[42] A. Rehman, A. Hussain, and S. Nadeem, "Assisting and opposing stagnation point pseudoplastic nano liquid flow towards a flexible riga sheet: a computational approach," *Mathematical Problems in Engineering*, vol. 2021, Article ID 6610332, 14 pages, 2021.

[43] A. Rehman, A. Hussain, and S. Nadeem, "Physical aspects of convective and radiative molecular theory of liquid originated nanofluid flow in the existence of variable properties," *Physica Scripta*, vol. 96, no. 3, 2020.